



## Special issue of the journal “Condensed Matter and Interphases”: “Physicochemical Analysis in Materials Science” (continued)

### Review

Review article

<https://doi.org/10.17308/kcmf.2025.27/12483>

## Features of synthesis and properties of new materials based on monoisotopic silicon and germanium. Review

A. D. Bulanov<sup>1</sup>, V. A. Gavva<sup>1</sup>, O. Yu. Troshin<sup>1</sup>✉

<sup>1</sup>G. G. Devyatykh Institute of Chemistry of High-Purity Substances, Russian Academy of Sciences, 49 Tropinina st., Nizhny Novgorod 603951 Russian Federation

### Abstract

This paper reviews scientific works on the preparation and properties of isotopically enriched silicon and germanium, along with their compounds. It covers the technological aspects and peculiarities of synthetic methods with the deep purification processes for obtaining isotopically enriched silicon and germanium compounds. The review also discusses the production of polycrystalline and single-crystal samples with varying degrees of isotopic and chemical purity. The results of a study investigating the physicochemical characteristics of both simple and complex substances derived from isotopically enriched silicon and germanium are presented. These studies indicate that the isotopic composition of silicon and germanium significantly affects heat capacity, thermal conductivity, and light absorption processes. Finally, the paper explores current applications of substances and materials based on isotopically enriched silicon and germanium.

**Keywords:** Silicon, Germanium, Isotopes, Hydrides, Materials

**Funding:** The study was supported by the Ministry of Science and Education of the Russian Federation within the framework of the government order, FFSR-2022-0003.

**For citation:** Bulanov A. D., Gavva V. A., Troshin O. Yu. Features of synthesis and properties of new materials based on monoisotopic silicon and germanium. Review. *Condensed Matter and Interphases*. 2025;27(1): 3–15. <https://doi.org/10.17308/kcmf.2025.27/12483>

**Для цитирования:** Буланов А. Д., Гавва В. А., Трошин О. Ю. Особенности синтеза и свойства новых материалов на основе моноизотопных кремния и германия. Обзор. *Конденсированные среды и межфазные границы*. 2025;27(1): 3–15. <https://doi.org/10.17308/kcmf.2025.27/12483>

✉ Oleg Yu. Troshin, e-mail: [troshin@ihps-nnov.ru](mailto:troshin@ihps-nnov.ru)

© Bulanov A. D., Gavva V. A., Troshin O. Yu., 2025



The content is available under Creative Commons Attribution 4.0 License.

Conventionally, the characteristics that determine the set of physical and chemical properties of substances and materials include morphology, the level of chemical purity, and structural perfection. However, as a rule, the presence of several isotopes in the natural composition of most chemical elements is often ignored. Yet, these isotopes can be considered as a combination of the main and impurity isotopes of the chemical element [1, 2].

Differences in the properties of isotopically modified substances (the so-called isotopic effect) are due to the difference in the molar masses of isotopes. What is more, they are more noticeable in the chemical elements in periods 1–2 of the Mendeleev periodic table [3]. A detailed study and expansion of the database of properties of individual isotopes of chemical elements in the form of simple substances and compounds is important for fundamental and applied science. This information is relevant for predicting the properties and for the manufacturing of isotopic compositions, i.e. mixtures with desired properties, as part of isotopic engineering [4].

In the case of chemical elements with a relatively small difference in the mass numbers of isotopes, it is necessary to obtain corresponding substances with high chemical purity and structural perfection which will allow a definitive determination of the isotopic effects. High-tech semiconductor materials, monocrystalline silicon and germanium, are the most convenient for the study of isotopic effects. They are currently considered as the most advanced materials in terms of structural perfection and chemical purity.

Silicon is represented in nature by three stable isotopes:  $^{28}\text{Si}$  (92.230%),  $^{29}\text{Si}$  (4.683%), and  $^{30}\text{Si}$  (3.087%). Among the radioactive isotopes of silicon,  $^{32}\text{Si}$  ( $T_{1/2} \sim 150$  years) is the longest-lasting [3]. Germanium consists of four stable isotopes,  $^{70}\text{Ge}$  (20.84%),  $^{72}\text{Ge}$  (27.54%),  $^{73}\text{Ge}$  (7.73%),  $^{74}\text{Ge}$  (36.28%), and  $^{76}\text{Ge}$  (7.61%), with a half-life of about  $2 \cdot 10^{21}$  years [3]. Gas ultracentrifugation of volatile fluorides is mainly used to separate the isotopes of these chemical elements [5–7]; monogermane is also used in the separation of germanium isotopes [8, 9].

The first works dedicated to the production and properties of monoisotopic silicon and germanium were published in the 1990s. In paper

[10] the Czochralski technique with a natural silicon seed was used to produce a single crystal of silicon-28 with a weight of about 300 g and an isotope content of  $^{28}\text{Si}$  at 99 mol %. This single crystal was used to measure the parameter of the silicon-28 lattice and to determine the Avogadro's number. The initial silicon-28 was obtained by aluminum reduction of silicon dioxide-28 with a 99.88% silicon-28 enrichment. The content of oxygen, carbon, and boron impurities in silicon-28 was  $10^{16} - 10^{18}$  atoms/cm<sup>3</sup>. The authors of [11] obtained a single crystal of silicon-28 with a diameter of 4 mm and a length of 50 mm and a 99.924 at. % isotope content of  $^{28}\text{Si}$ . The silicon powder obtained by the aluminum reduction of silicon oxide-28 was compressed, sintered, and zone-melted. The resulting sample had a *p*-type conductivity and contained an aluminum impurity at  $1 \cdot 10^{-3}$  at. %. According to the authors, isotopically enriched silicon was a promising material for the development of a quantum computer.

In [12], the liquid-phase epitaxy was used to obtain a film of silicon-28 with a 99.7% enrichment and a thickness of 11.7 microns from the indium melt. The film was produced on a natural silicon substrate, on which an aluminum layer with a thickness of about 1000 Å was sprayed. After measuring the thermal conductivity of the sample, it was found that the thermal conductivity of isotopically enriched  $^{28}\text{Si}$  at 298 K was about 60% higher than that of silicon with a natural isotopic composition. However, as a result of interlaboratory measurements using the technique of stationary heat flux, it was found that the difference in the thermal conductivity of isotopically enriched  $^{28}\text{Si}$  and natural silicon did not exceed  $10 \pm 2\%$  [13]. The significant discrepancy in the value of the thermal conductivity of silicon-28 obtained in [12] could be due to the contamination of the sample.

The researchers also obtained isotopically enriched samples of  $^{29}\text{Si}$  and  $^{30}\text{Si}$  in the form of single crystals [5,14] and epitaxial films [15] with the degree of enrichment in the main isotope of silicon that did not exceed 99.9%. In [5], polycrystalline silicon-29 and silicon-30 were produced by the thermal decomposition of monosilane which had been obtained by the reaction between silicon tetrafluoride ( $^{29}\text{SiF}_4$ ,

$^{30}\text{SiF}_4$ ) and calcium hydride. Monoisotopic silicon was deposited on a molybdenum wire, resulting in granules with a size of 0.3 – 0.5 mm. To minimize isotopic dilution at the stage of growing single crystals by the Czochralski technique, small-volume crucibles with a coating of  $^{29}\text{SiO}_2$  or  $^{30}\text{SiO}_2$  with a thickness of 100-150 microns were used. The content of the main isotope of silicon in the obtained  $^{29}\text{Si}$  and  $^{30}\text{Si}$  single crystals was  $99.225 \pm 0.023$  at. % and  $99.742 \pm 0.015$  at. %; in the initial  $^{29}\text{SiF}_4$  and  $^{30}\text{SiF}_4$ , the content of  $^{29}\text{Si}$ ,  $^{30}\text{Si}$  in the composition of silicon was  $99.576 \pm 0.105$  at. % and  $99.829 \pm 0.060$  at. %. In [14], silicon-29 was precipitated on a graphite substrate, after the removal of which the resulting silicon-29 was melted into a rod. A natural silicon seed was used to produce a single crystal of silicon-29.

The authors of [16] measured the temperature dependence of the thermal conductivity of a single crystal of isotopically enriched silicon-29 (99.919%) in the range of 2.4 - 410 K. It was found that at low temperatures ( $T < 6$  K) in the mode of boundary phonon scattering, the thermal conductivity of the  $^{29}\text{Si}$  crystal was higher than that of the  $^{28}\text{Si}$  crystal (99.983%). In the high temperature region, where thermal conductivity is determined by anharmonic processes of phonon scattering, the value of thermal conductivity of  $^{29}\text{Si}$  was lower than that of  $^{28}\text{Si}$ .

To obtain significant quantities of silicon-28, as well as samples of silicon-29 and silicon-30, the Institute of Chemistry of High Purity Substances of the Russian Academy of Sciences developed a laboratory technology for the synthesis, deep purification, and thermal decomposition of monosilane for the production of polycrystalline silicon-28 [1,2]. Further studies aimed at obtaining and improving the isotopic and chemical purity were triggered by using monoisotopic silicon-28 to determine the Avogadro's number and creating a physically justified kilogram standard within the framework of the *Avogadro* and *Kilogram* projects [6, 7, 10, 17, 18]. Silicon tetrafluoride  $\text{SiF}_4$  was used as the starting material. It was enriched by gas ultracentrifugation (ZAO *Tsentrotekh-SPb*, AO *Production Association "Electrochemical Plant"*) to the content of silicon-28 of over 99.99% [7]. The content of molecular impurities in samples of isotopically enriched  $^{28}\text{SiF}_4$  according to high-resolution Fourier IR spectroscopy [19]

and gas chromatography [20] was:  $\text{Si}_2\text{F}_6\text{O} - 2 \cdot 10^{-1}$  mol %;  $\text{CO}_2 - 1 \cdot 10^{-2}$  mol %;  $\text{H}_2\text{O} - 6 \cdot 10^{-3}$  mol %;  $\text{HF} - 3 \cdot 10^{-4}$  mol %; hydrocarbons  $\text{C}_1\text{-C}_4$  (methane, ethane, ethylene, propane, butane) –  $n \cdot 10^{-3}$  –  $n \cdot 10^{-5}$  mol % [21]. The content of metal impurities in isotopically enriched silicon tetrafluoride, determined by the atomic emission with matrix distillation for the concentration of non-volatile impurities, was at  $n \cdot 10^{-7}$  wt. % [22, 23]. The content of silicon isotopes in the composition of silicon tetrafluoride, as well as monosilane and crystalline silicon, was determined by mass spectrometry [24].

$^{28}\text{SiH}_4$  was synthesized by the reaction of  $^{28}\text{SiF}_4$  with ground calcium hydride in a hydrogen flow reactor. Calcium hydride was synthesized from distilled calcium and hydrogen [25] and ground before the synthesis (*in situ*); calcium hydride was ground to a particle size of less than 1 mm and was loaded into the monosilane synthesis reactor in boxes with an inert nitrogen atmosphere. This ensured a low content of oxygen-containing impurities in calcium hydride, which are formed upon contact with atmospheric moisture, and a high isolated yield of monosilane. The productivity of the laboratory synthesis was 3 kg of  $^{28}\text{SiH}_4$  per month. However, this technique for monosilane synthesis has a disadvantage, i.e. the low degree of conversion of the solid-phase reagent,  $\text{CaH}_2$ , which does not exceed 15% [26]. Therefore, it is important to increase the degree of conversion of calcium hydride. One of the solutions can be to carry out the conversion process at an elevated pressure [27] or to use mechanical activation, i.e. grinding the solid-phase reagent in the process of producing monosilane in a rotating flow reactor [28].

The isolated yield of  $^{28}\text{SiH}_4$  over  $^{28}\text{SiF}_4$  was 92–96%. According to [26], the obtained monosilane contains impurities of hydrocarbons, siloxanes, and polysilanes at  $n \cdot 10^{-3} - n \cdot 10^{-5}$  mol %. One of the sources of hydrocarbon impurities in monosilane is the hydrogenation of impurity carbon in calcium during the contact of calcium hydride with hydrogen at an elevated temperature [21]. Preliminary purging of the reactor with calcium hydride with high-purity hydrogen at 200 °C allows reducing the content of unsaturated hydrocarbons in the resulting silane and disiloxane impurities by about an order of magnitude [29].

A combination of cryofiltration and low-temperature rectification was used for deep purification of isotopically enriched monosilane [30]. Cryofiltration on a Petryanov filter at a temperature of about 165 K allowed separating the higher-boiling impurities of siloxanes and higher silanes (disilane, trisilane). Rectification was carried out in metal rectification columns with a middle feeding tank in the mode of discrete choice of impurities from the lower and upper sections filled with a nichrome wire spiral-prismatic nozzle [29]. The yield of the high-purity product at the purification stages was 80–90%. The content of chemical impurities in samples of high-purity monosilane was: alkylsilanes at  $n \cdot 10^{-6}$  mol %, hydrocarbons  $C_1$ - $C_9$  at  $n \cdot 10^{-5}$  mol %, disiloxane at  $10^{-3}$  mol %, and higher silanes at  $n \cdot 10^{-2}$  mol %.

Monoisotopic polycrystalline silicon ( $^{28}\text{Si}$ ,  $^{29}\text{Si}$ ,  $^{30}\text{Si}$ ) was obtained by the pyrolysis of high-purity isotopically enriched monosilane in SAA-20 and SAA-800 monosilane decomposition plants (Steremat Electrowarme), which differed in the maximum amount of obtained material (150 g and 6 kg, respectively). In the absence of rods from isotopically enriched material and due to the restrictions regarding the usage of silicon rods of natural isotopic composition to avoid isotopic dilution, monoisotopic silicon was deposited on molybdenum substrates. This involved obtaining silicon polycrystals, which were connected into a tape by means of contactless high-frequency welding. The resulting tape was used as a substrate for silicon precipitation [31]. Thin walled stainless steel tubes (12X18H10T) can also be used as a substrate for precipitation. After precipitation, the substrate material dissolved in hydrochloric acid and the resulting silicon tube was melted into a rod of the specified diameter by crucibleless melting. This technique is simpler and reduces the cost for the production of seed rods, which is especially important when obtaining samples of monoisotopic silicon of various nature and variable isotopic composition.

The manufacture of monocrystalline silicon samples involved using crucibleless melting and the Czochralski technique. To avoid isotopic dilution when using the Czochralski technique with quartz crucibles, special techniques were developed for applying protective coatings from

isotopically enriched silicon dioxide by oxidizing monosilane  $^{28}\text{SiH}_4$  [32].

One of the results of the *Avogadro* international project was the production of two spheres of monocrystalline silicon-28 with a diameter of 96.3 mm and a mass of 1 kg. Measuring its volume, density, atomic lattice constant, and molar mass allowed obtaining the Avogadro constant,  $N_A = 6.022\,14082(18) \cdot 10^{23}$  mol $^{-1}$  with a relative error of  $2 \cdot 10^{-8}$  [7].

The properties of isotopically enriched silicon samples are presented in [13,16,33–41] and generalized in [2]. The difference in the properties of samples of monoisotopic silicon and silicon of the natural isotopic composition is associated with a different value of the average atomic mass and with an uneven distribution of isotopes in the sample. A number of properties dependent on spin interactions (nuclear magnetic resonance spectra, electron paramagnetic resonance, and the parameters of spin-spin and spin-lattice interactions) are affected by the concentration of silicon-29 with a non-zero nuclear spin. Table 1 shows the properties of monocrystalline samples of  $^{28}\text{Si}$ ,  $^{29}\text{Si}$ , and  $^{30}\text{Si}$  and pure silicon of the natural isotopic composition  $^{\text{nat}}\text{Si}$  [2].

Samples of isotopically enriched germanium were obtained using a hydride technology [42]. Unlike the production of silicon isotopes, germanium did not require converting the working gas into volatile hydride for ultracentrifugation. Monogermane was used to separate germanium isotopes [8]. The technique for obtaining high-purity germanium isotopes included the stages of low-temperature rectification and thermal decomposition of monogermane and additional purification of germanium by zone melting [9]. Rectification purification of monogermanes was carried out on a metal column with a middle cube, equipped with an automated refrigerant supply system and a gas chromatograph for operational control of the impurity composition of the fractions. The weight of the monogermane loaded into the column was about 250 g, the duration of purification was about 40 hours, the isolated yield of the rectified product was 75–80%. The content of molecular impurities ( $C_1$ - $C_9$  hydrocarbons and their halogen derivatives, alkyl and halogen germanes, etc.) in purified monogermane samples according to chromatography-mass spectrometry [43] was at  $n \cdot 10^{-5}$  –  $n \cdot 10^{-6}$  mol %.



**Table 1.** Properties of samples of  $^{28}\text{Si}$ ,  $^{29}\text{Si}$ ,  $^{30}\text{Si}$  and high-purity silicon of natural isotopic composition  $^{\text{nat}}\text{Si}$  [2]

Property	Sample				The content of the main isotope, %
	$^{28}\text{Si}$	$^{29}\text{Si}$	$^{30}\text{Si}$	$^{\text{nat}}\text{Si}$	
Density at 20 °C, $\text{g}\cdot\text{cm}^{-3}$	2.320071	–	–	2.329045	$^{28}\text{Si}$ – 99.99
Debye temperature, K	641	627	616	638	$^{28}\text{Si}$ – 99.98 $^{29}\text{Si}$ – 99.0 $^{30}\text{Si}$ – 99.0
Heat capacity at 100 K, $\text{J}\cdot\text{mol}^{-1}\cdot\text{K}^{-1}$	7.24	7.40	7.61	7.24	$^{28}\text{Si}$ – 99,98 $^{29}\text{Si}$ – 99,0 $^{30}\text{Si}$ – 99,0
Thermal conductivity at 25 K, $\text{W}\cdot\text{cm}^{-1}\cdot\text{K}^{-1}$	288	214	–	45.6	$^{28}\text{Si}$ – 99.98 $^{29}\text{Si}$ – 99.92
Raman shift at 20 °C, $\text{cm}^{-1}$	521.4	512.3	503.9	520.8	$^{28}\text{Si}$ – 99.993 $^{29}\text{Si}$ – 99.92 $^{30}\text{Si}$ – 99.97
Refractive index at 293 K, $\lambda=1.5$ microns	3.48207	3.48171	3.48112	3.48191	$^{28}\text{Si}$ – 99.993 $^{29}\text{Si}$ – 99.92 $^{30}\text{Si}$ – 99.97

Thermal decomposition of monogermane was performed at a temperature of 500 °C in a quartz tube with a pyrocarbon coating. As a result of the monogermane decomposition, polycrystalline and powdered germanium was formed in the reactor, which was then melted into an ingot; the isolated yield of germanium was about 95%. Additional purification of monoisotopic germanium was carried out by zone melting in quartz boats coated with amorphous silicon dioxide in the pure hydrogen atmosphere. Germanium single crystals were grown by the Bridgman technique and the Czochralski technique [2, 5–7].

When crystals of isotopically enriched germanium are grown by the Czochralski technique, there is a problem associated with the lack of oriented isotopically enriched monocrystalline seeds. Growing single crystals of isotopically enriched germanium using a germanium seed of a natural isotopic composition leads to isotopic dilution, which can reach  $n\cdot 10^{-1}\%$ . To reduce the isotopic dilution of germanium, crystals were grown stage by stage: the first stage involved growing in a quartz crucible a single crystal with a diameter of 5 mm and a length of 50 mm on a seed from germanium of a natural isotopic composition using a small amount of melt of isotopically enriched germanium. This single crystal was then used as a seed for growing a single crystal of isotopically enriched

germanium. It is also possible to use a seed from previously obtained isotopically enriched germanium to minimize a certain germanium isotope. For example, when obtaining a single crystal of germanium-70, germanium-74 was used as a seed [42].

The isotopic composition of germanium in samples of isotopically enriched monogermane and germanium was determined by mass spectrometry [44]. To date, the Institute of Chemistry of High Purity Substances of the Russian Academy of Sciences have obtained and described all stable isotopes of germanium with a content of the main substance of over 99% [42, 45]. Table 2 shows the isotopic composition of germanium in high-purity monogermanes and isotopically enriched germanium [2, 42].

Some properties of the samples of isotopically enriched germanium and its hydrides were studied in [46–53].

In [46], differential scanning calorimetry was used to determine the melting point for the samples of germanium isotopes  $^{72}\text{Ge}$ ,  $^{73}\text{Ge}$ ,  $^{74}\text{Ge}$ , and  $^{76}\text{Ge}$  with the content of the main isotope of 99.98439%, 99.8995%, 99.9365%, and 88.21%, respectively. It was established that the melting point of samples of isotopically enriched germanium decreased with an increase in the atomic mass of the isotope. The change was 0.15 K per unit of atomic mass, which is

**Table 2.** The content of germanium isotopes in the composition of the obtained samples of high-purity monogermans and isotopically enriched germanium

Sub-stance	The content of the germanium isotope, at. %				
	<sup>70</sup> Ge	<sup>72</sup> Ge	<sup>73</sup> Ge	<sup>74</sup> Ge	<sup>76</sup> Ge
<sup>70</sup> GeH <sub>4</sub>	99.99303±0.00012	0.00678±0.00009	0.00005±0.00003	0.00012±0.00005	<0.00001
<sup>70</sup> Ge	99.99329±0.00006	0.00669±0.00005	0.00002±0.00001	0.00001	0.00001
<sup>72</sup> GeH <sub>4</sub>	0.005±0.001	99.953±0.008	0.018±0.003	0.023±0.006	0.002±0.001
<sup>72</sup> Ge	0.00009±0.00002	99.98439±0.00091	0.01191±0.00073	0.00356±0.00030	0.00005±0.00001
<sup>73</sup> GeH <sub>4</sub>	0.0012±0.0005	0.0415±0.0080	99.8942±0.0100	0.0626±0.0100	0.0005±0.0003
<sup>73</sup> Ge	0.0001±0.0001	0.0391±0.0027	99.8995±0.0155	0.0611±0.0102	0.0002±0.0001
<sup>74</sup> GeH <sub>4</sub>	0.0007±0.0003	0.0017±0.0004	0.059±0.003	99.9377±0.0031	0.0033±0.0006
<sup>74</sup> Ge	0.0001±0.0001	0.0009±0.0004	0.0595±0.0010	99.9365±0.0011	0.0030±0.0003
<sup>76</sup> GeH <sub>4</sub>	0.12±0.01	0.17±0.01	0.07±0.01	11.50±0.50	88.14±0.55
<sup>76</sup> Ge	0.060±0.009	0.090±0.009	0.051±0.009	11.592±0.192	88.207±0.188

qualitatively consistent with the value calculated by the Lindemann's formula, taking into account the effect of "isotopic compression" of the unit cell. The dependence of the melting point  $T_m$  (°C) on the average atomic mass  $M$  can be described by the equation  $T_m = 949.3 - 0.153 \cdot M$ .

In [47], differential scanning calorimetry was used to remeasure the melting point of the samples studied in [46] <sup>72</sup>Ge, <sup>73</sup>Ge, <sup>74</sup>Ge, and <sup>76</sup>Ge and to measure the melting point of the sample of germanium-70 with a content of the main isotope of 99.99329%. The melting point for samples <sup>70</sup>Ge, <sup>72</sup>Ge, <sup>73</sup>Ge, <sup>74</sup>Ge, and <sup>76</sup>Ge was 1,212.0 K, 1,211.6 K, 1,211.3 K, 1,211.1 K, and 1,210.8 K, respectively.

The temperature dependence of the thermal conductivity of single crystals of isotopically enriched germanium <sup>70</sup>Ge (degree of enrichment 99.926%), <sup>72</sup>Ge (99.980%), <sup>74</sup>Ge (99.921%) in the temperature range of 80–310 K was measured in [48]. In the studied temperature range, the thermal conductivity of germanium was determined by anharmonic processes of phonon scattering. A decrease in the value of thermal conductivity was also experimentally observed with an increase in the mass of the germanium isotope.

Optical spectroscopy was used to study the optical transmission of the germanium isotopes <sup>70</sup>Ge, <sup>72</sup>Ge, <sup>73</sup>Ge, <sup>74</sup>Ge, and <sup>76</sup>Ge in the terahertz spectral range of up to 3,000  $\mu\text{m}$  [49]. It was shown that the minimum absorption within the wavelength range of 30–3,000  $\mu\text{m}$  was within the range of 200–800  $\mu\text{m}$ , and the corresponding

absorption coefficient for this range was less than  $1 \text{ cm}^{-1}$  for most of the studied monocrystalline samples. Within the range of 1,000–3,000  $\mu\text{m}$ , there was a trend towards an increase in the absorption coefficient with an increase in the mass number of the germanium isotope.

Paper [50] presents the results of the precision measurement of the refractive index of stable single crystals of germanium isotopes <sup>72</sup>Ge, <sup>73</sup>Ge, <sup>74</sup>Ge, and <sup>76</sup>Ge with high enrichment by Fourier transform interference refractometry in the range of 1.94–20  $\mu\text{m}$  with a resolution of  $0.1 \text{ cm}^{-1}$ . This paper provides coefficients of the generalized Cauchy dispersion function, approximating experimental values for the refractive index over the entire measurement range, and the transmission and Raman light scattering spectra.

The authors of [51] conducted a single experiment to investigate the dependence of the position of phonon absorption peaks in the range of 11–40  $\mu\text{m}$  for five single-crystal samples of germanium, <sup>70</sup>Ge, <sup>72</sup>Ge, <sup>73</sup>Ge, <sup>74</sup>Ge, and <sup>76</sup>Ge. The obtained dependence can be used to identify the nature of single crystals of isotopically enriched germanium [52].

The authors of [53] calculated the standard thermodynamic functions of isotopically enriched monogermans, <sup>70</sup>GeH<sub>4</sub>, <sup>72</sup>GeH<sub>4</sub>, <sup>73</sup>GeH<sub>4</sub>, <sup>74</sup>GeH<sub>4</sub>, and <sup>76</sup>GeH<sub>4</sub> in the temperature range of 200–700 K in the approximations "harmonic generator – rigid rotator", "anharmonic generator – oscillating non-rigid rotator", as well as by the direct

summation of experimental energy values. They established the influence of the isotopic effect on the values of the standard isobaric heat capacity, entropy, enthalpy of heating and the reduced isobaric-isothermal potential of germanium. The authors formulated the limiting requirements for the accuracy of spectral parameters used to identify the influence of the isotopic effect on thermodynamic functions and interatomic distances in the germane molecule.

In addition to fundamental and metrological studies, isotopically enriched silicon and germanium, monosilane and monogermane were investigated in the works dedicated to creating prototypes of quantum devices. State and private programs for the development and application of quantum devices are run in many countries all over the world [54]. In Russia, the systematic development of quantum technologies is carried out according to the Roadmap for the Development of the High-Tech Area “Quantum Computing” [55], which provides for various approaches to the implementation of quantum devices. One of the most promising areas is the model of a solid-state quantum computer using the state of the nuclear spin of an atom as a carrier of quantum information, a qubit [56]. An ensemble of qubits is created by implanting atoms of elements with a non-zero nuclear spin into a crystalline matrix. In the case of silicon, these are atoms of silicon-29 (nuclear spin 1/2+) distributed in a crystalline matrix of silicon-28 atoms, while in the case of germanium, these are atoms of germanium-73 (nuclear spin 9/2+) in a matrix of atoms of a common isotope ( $^{70}\text{Ge}$ ,  $^{72}\text{Ge}$ ,  $^{74}\text{Ge}$ ). Of interest are heterostructures based on silicon

and germanium isotopes [57], for the creation of which molecular beam epitaxy and vapor deposition methods are used. The precursors for the production of epitaxial structures by molecular beam epitaxy are elementary silicon and germanium, whereas their volatile hydrides are the precursors for chemical vapor deposition (monosilane and monogermane).

To establish the influence of the degree of isotopic enrichment on the performance of silicon-based qubits in order to determine the limiting, physically justified values of silicon and germanium enrichment for the creation of qubits, we need isotopically enriched substances (silicon, germanium, monosilane, and monogermane) with different isotope content of  $^{29}\text{Si}$ ,  $^{73}\text{Ge}$ . Samples of these isotopically enriched substances were prepared according to the techniques described above. Isotopically enriched silicon tetrafluoride with the content of the main isotope  $^{28}\text{Si}$  at 99.9%, 99.99%, 99.999% and monogermane with the content of the main isotope  $^{72}\text{Ge}$  at 99.9% were used as starting substances [58].

Table 3 shows the content of silicon isotopes in the composition of samples of  $^{28}\text{SiF}_4$ ,  $^{28}\text{SiH}_4$ ,  $^{28}\text{Si}$  with different levels of enrichment.

From Table 3, it can be concluded that there was a statistically significant dilution of sample N°3 with an isotopic enrichment of 99.999% at the stage of silicon-28 tetrafluoride conversion to monosilane, which may be due to the intake of  $^{29}\text{Si}$ ,  $^{30}\text{Si}$  from the material of the synthesis equipment or storage tanks.

Table 4 provides information on the content of impurities of a number of substances (hydrocarbons, halogen derivatives

**Table 3.** The content of silicon isotopes in samples of isotopically enriched silicon tetrafluoride-28 with different levels of enrichment

Sample		The content of the silicon isotope, wt. %		
		$^{28}\text{Si}$	$^{29}\text{Si}$	$^{30}\text{Si}$
N°1 (3N)	$^{28}\text{SiF}_4$	99.96034±0.00160	0.03957±0.00160	0.00009±0.00006
	$^{28}\text{SiH}_4$	99.9668±0.0015	0.0329±0.0015	0.0003±0.0001
	$^{28}\text{Si}$	99.9657±0.0015	0.0340±0.0008	0.0003±0.0001
N°2 (4N)	$^{28}\text{SiF}_4$	99.99623±0.00022	0.00369±0.00022	0.00008±0.00002
	$^{28}\text{SiH}_4$	99.99577±0.00028	0.00418±0.00028	0.00005±0.00001
	$^{28}\text{Si}$	99.99581±0.00045	0.00411±0.00043	0.00008±0.00002
N°3 (5N)	$^{28}\text{SiF}_4$	99.99917±0.00011	0.00080±0.00011	0.00003±0.00001
	$^{28}\text{SiH}_4$	99.99882±0.00010	0.00112±0.00010	0.00006±0.00001
	$^{28}\text{Si}$	99.99881±0.00010	0.00114±0.00010	0.00005±0.00001

**Table 4.** The content of molecular impurities in high-purity  $^{28}\text{SiH}_4$ 

Impurity	Content, % mol.	Impurity	Content, % mol.
Ar	$(4.3 \pm 0.6) \cdot 10^{-5}$	trans-1,2-C <sub>2</sub> H <sub>2</sub> F <sub>2</sub>	$< 5 \cdot 10^{-7}$
CO <sub>2</sub>	$< 2 \cdot 10^{-6}$	cis-1,2-C <sub>2</sub> H <sub>2</sub> F <sub>2</sub>	$< 4 \cdot 10^{-7}$
CH <sub>4</sub>	$< 5 \cdot 10^{-6}$	1,1,1,2-C <sub>2</sub> H <sub>2</sub> F <sub>4</sub>	$< 5 \cdot 10^{-7}$
C <sub>2</sub> H <sub>2</sub>	$< 2 \cdot 10^{-6}$	1,1,2,2-C <sub>2</sub> H <sub>2</sub> F <sub>4</sub>	$< 5 \cdot 10^{-7}$
C <sub>2</sub> H <sub>4</sub>	$< 2 \cdot 10^{-6}$	CH <sub>3</sub> Cl	$< 5 \cdot 10^{-7}$
C <sub>2</sub> H <sub>6</sub>	$< 2 \cdot 10^{-6}$	CF <sub>3</sub> Cl	$< 5 \cdot 10^{-7}$
C <sub>3</sub> H <sub>6</sub>	$< 2 \cdot 10^{-6}$	Si <sub>2</sub> H <sub>6</sub> O	$< 2 \cdot 10^{-6}$
C <sub>3</sub> H <sub>8</sub>	$< 1 \cdot 10^{-6}$	Si <sub>3</sub> H <sub>8</sub> O <sub>2</sub>	$(1.3 \pm 0.4) \cdot 10^{-6}$
<i>i</i> -C <sub>4</sub> H <sub>10</sub>	$< 2 \cdot 10^{-6}$	<i>i</i> -Si <sub>4</sub> O <sub>3</sub> H <sub>10</sub>	$< 2 \cdot 10^{-7}$
<i>n</i> -C <sub>4</sub> H <sub>10</sub>	$< 2 \cdot 10^{-6}$	<i>n</i> -Si <sub>4</sub> O <sub>3</sub> H <sub>10</sub>	$< 2 \cdot 10^{-7}$
C <sub>4</sub> H <sub>8</sub> 1-buten	$< 2 \cdot 10^{-6}$	Si <sub>2</sub> OH <sub>4</sub> F <sub>2</sub>	$< 7 \cdot 10^{-7}$
C <sub>4</sub> H <sub>8</sub> 2-buten	$< 2 \cdot 10^{-6}$	Si <sub>2</sub> OH <sub>5</sub> F	$(1.8 \pm 0.5) \cdot 10^{-6}$
<i>n</i> -C <sub>5</sub> H <sub>12</sub>	$< 2 \cdot 10^{-6}$	Si <sub>3</sub> O <sub>2</sub> H <sub>6</sub> F <sub>2</sub>	$< 3 \cdot 10^{-7}$
<i>n</i> -C <sub>6</sub> H <sub>14</sub>	$< 2 \cdot 10^{-6}$	Si <sub>3</sub> O <sub>2</sub> H <sub>7</sub> F	$< 4 \cdot 10^{-7}$
<i>n</i> -C <sub>7</sub> H <sub>16</sub>	$< 2 \cdot 10^{-6}$	Si <sub>2</sub> H <sub>6</sub>	$< 3 \cdot 10^{-6}$
<i>n</i> -C <sub>8</sub> H <sub>18</sub>	$< 5 \cdot 10^{-6}$	Si <sub>3</sub> H <sub>8</sub>	$< 6 \cdot 10^{-7}$
C <sub>6</sub> H <sub>6</sub>	$< 1 \cdot 10^{-6}$	<i>i</i> -Si <sub>4</sub> H <sub>10</sub>	$< 6 \cdot 10^{-7}$
C <sub>6</sub> H <sub>5</sub> -CH <sub>3</sub>	$< 4 \cdot 10^{-7}$	<i>n</i> -Si <sub>4</sub> H <sub>10</sub>	$< 3 \cdot 10^{-7}$
GeH <sub>4</sub>	$< 3 \cdot 10^{-6}$	<i>i</i> -Si <sub>5</sub> H <sub>12</sub>	$< 3 \cdot 10^{-6}$
PH <sub>3</sub>	$< 1 \cdot 10^{-6}$	<i>n</i> -Si <sub>5</sub> H <sub>12</sub>	$< 3 \cdot 10^{-6}$
AsH <sub>3</sub>	$< 3 \cdot 10^{-6}$	CH <sub>3</sub> SiH <sub>3</sub>	$< 1 \cdot 10^{-6}$
H <sub>2</sub> S	$< 5 \cdot 10^{-6}$	C <sub>2</sub> H <sub>5</sub> SiH <sub>3</sub>	$< 1 \cdot 10^{-6}$
CF <sub>4</sub>	$< 4 \cdot 10^{-7}$	(SiH <sub>3</sub> ) <sub>2</sub> CH <sub>2</sub>	$< 3 \cdot 10^{-7}$
CHF <sub>3</sub>	$< 5 \cdot 10^{-6}$	(CH <sub>3</sub> ) <sub>3</sub> SiH	$< 5 \cdot 10^{-7}$
C <sub>2</sub> F <sub>4</sub>	$< 3 \cdot 10^{-7}$	(C <sub>2</sub> H <sub>5</sub> ) <sub>2</sub> SiH <sub>2</sub>	$< 6 \cdot 10^{-7}$
1,1,1-C <sub>2</sub> H <sub>3</sub> F <sub>3</sub>	$< 7 \cdot 10^{-7}$	Si <sub>2</sub> H <sub>5</sub> CH <sub>3</sub>	$< 1 \cdot 10^{-6}$

of hydrocarbons, siloxanes, homologues of monosilane, and hydrides of a number of chemical elements) in an isotopically enriched monosilane – rectifier  $^{28}\text{SiH}_4$ , according to the chromatography-mass spectrometry data.

Fig. 1 shows an image of a sample of a single-crystal silicon-28 (content of the main isotope 99.9988 wt. %) weighing 90 g.

Table 5 shows the content of germanium isotopes in the composition of samples of isotopically enriched monogermane  $^{72}\text{GeH}_4$  and germanium-72 obtained from it according to inductively coupled plasma mass spectrometry.

From Table 5, it can be concluded that there is no statistically significant isotopic dilution at the stage of obtaining crystalline germanium-72.

**Fig. 1.** Image of a single crystal silicon sample – 28

Table 6 provides information on the content of a number of impurities (hydrocarbons, halogen derivatives of hydrocarbons, siloxanes, homologues of monosilane, hydrides of a number of chemical elements) in isotopically enriched monogermane – rectifier  $^{72}\text{GeH}_4$  according to chromatography-mass spectrometry data.



**Table 5.** The content of germanium isotopes in the composition of isotopically enriched monogermane samples  $^{72}\text{GeH}_4$  and germanium-72

Substance	The content of the germanium isotope, wt. %				
	$^{70}\text{Ge}$	$^{72}\text{Ge}$	$^{73}\text{Ge}$	$^{74}\text{Ge}$	$^{76}\text{Ge}$
$^{72}\text{GeH}_4$	0.00035±0.00007	99.98460±0.00020	0.01140±0.00015	0.00357±0.00012	0.00008±0.00004
$^{72}\text{Ge}$	0.00011±0.00002	99.98576±0.00105	0.01099±0.00096	0.00310±0.00030	0.00004±0.00001

**Table 6.** The content of molecular impurities in high-purity monogermane  $^{72}\text{GeH}_4$ 

Impurity	Impurity content, mol. %	Impurity	Impurity content, mol. %
Ar	$(2.8\pm 0.3)\cdot 10^{-5}$	i-C <sub>4</sub> H <sub>10</sub>	$< 2\cdot 10^{-6}$
CO <sub>2</sub>	$(3\pm 1)\cdot 10^{-6}$	n-C <sub>5</sub> H <sub>12</sub>	$< 1\cdot 10^{-6}$
N <sub>2</sub> O	$< 2\cdot 10^{-6}$	n-C <sub>6</sub> H <sub>14</sub>	$< 1\cdot 10^{-6}$
Kr	$< 3\cdot 10^{-7}$	i-C <sub>7</sub> H <sub>16</sub>	$< 1\cdot 10^{-6}$
Xe	$< 3\cdot 10^{-7}$	C <sub>7</sub> H <sub>16</sub> 3-methylhexane	$< 1\cdot 10^{-6}$
SiH <sub>4</sub>	$< 1\cdot 10^{-6}$	n-C <sub>7</sub> H <sub>16</sub>	$< 9\cdot 10^{-7}$
PH <sub>3</sub>	$< 1\cdot 10^{-6}$	n-C <sub>8</sub> H <sub>18</sub>	$< 2\cdot 10^{-6}$
AsH <sub>3</sub>	$< 2\cdot 10^{-6}$	C <sub>6</sub> H <sub>6</sub>	$< 2\cdot 10^{-7}$
H <sub>2</sub> S	$< 3\cdot 10^{-6}$	C <sub>6</sub> H <sub>5</sub> CH <sub>3</sub>	$< 2\cdot 10^{-7}$
CH <sub>4</sub>	$< 1\cdot 10^{-5}$	C <sub>2</sub> H <sub>5</sub> Cl	$< 5\cdot 10^{-7}$
C <sub>2</sub> H <sub>2</sub>	$< 2\cdot 10^{-6}$	CH <sub>2</sub> Cl <sub>2</sub>	$< 5\cdot 10^{-7}$
C <sub>2</sub> H <sub>4</sub>	$< 1\cdot 10^{-6}$	2-C <sub>3</sub> H <sub>7</sub> Cl	$< 9\cdot 10^{-7}$
C <sub>2</sub> H <sub>6</sub>	$< 2\cdot 10^{-6}$	C <sub>4</sub> H <sub>9</sub> F	$< 4\cdot 10^{-6}$
C <sub>3</sub> H <sub>6</sub>	$< 1\cdot 10^{-6}$	C <sub>2</sub> H <sub>5</sub> GeH <sub>3</sub>	$< 1\cdot 10^{-5}$
C <sub>3</sub> H <sub>8</sub>	$< 1\cdot 10^{-6}$	C <sub>2</sub> H <sub>5</sub> Ge <sub>2</sub> H <sub>5</sub>	$< 1\cdot 10^{-5}$
C <sub>4</sub> H <sub>8</sub> 2-methyl-1-propen	$< 2\cdot 10^{-6}$	1,1,2-C <sub>2</sub> F <sub>3</sub> Cl <sub>3</sub>	$< 4\cdot 10^{-7}$
C <sub>4</sub> H <sub>8</sub> 1-buten	$< 2\cdot 10^{-6}$	1,1,2-C <sub>2</sub> H <sub>3</sub> Cl <sub>3</sub>	$< 6\cdot 10^{-7}$
C <sub>4</sub> H <sub>8</sub> 2-buten	$< 2\cdot 10^{-6}$	CH <sub>3</sub> GeH <sub>3</sub>	$< 1\cdot 10^{-6}$
n-C <sub>4</sub> H <sub>10</sub>	$< 2\cdot 10^{-6}$	CS <sub>2</sub>	$< 4\cdot 10^{-7}$

Currently, high-purity isotopically enriched monosilane and monogermane, as well as samples of monoisotopic silicon and germanium with a controlled content of isotopes with a non-zero nuclear spin, produced at the Institute of Chemistry of High Purity Substances of the Russian Academy of Sciences, are widely used in scientific research dedicated to the creation of quantum computing devices in Russia and abroad.

Research on the properties of isotopically enriched binary and complex substances is of fundamental scientific interest. Of particular interest is the production and study of the effect of the isotopic composition on the properties of optical materials, such as quartz glass. A theoretical evaluation provided in a number of works [59, 60] allows concluding that optical losses can be reduced and the optical fiber

transparency window can be expanded by the  $^{30}\text{Si}^{18}\text{O}_2$ -based light-conducting core and the  $^{28}\text{Si}^{16}\text{O}_2$ -based shell. According to the authors, it is also possible to ensure the effect of total internal reflection in such a quartz light-guiding structure due to the difference in the isotopic composition of silicon and oxygen without the use of alloying additives [4]. Silicon tetrachloride is used to obtain high-purity quartz glass by various techniques (vapor deposition, sol-gel method), while its tetrafluoride is used to separate silicon isotopes by gas centrifugation. For the synthesis of  $^{28}\text{SiCl}_4$ , a technique was developed which involves the conversion of isotopically enriched silicon tetrafluoride in static conditions using aluminum(III) chloride [61]; the isolated yield is about 95%, the productivity is 3–4 g of  $^{28}\text{SiCl}_4$ /hour. The reaction of silicon

tetrafluoride with aluminum(III) chloride proceeds successively with the formation of silicon fluoride-chlorides [62]; the equilibrium of liquid-vapor in the system  $\text{SiCl}_4 - \text{SiCl}_{4-n}\text{F}_n$  impurities ( $n = 1\div 4$ ) [63] was also studied. A technique has been developed for the synthesis of silicon-28 tetrachloride from simple substances in a quartz reactor (productivity 20 g/h), which, in combination with isothermal distillation, allows obtaining samples of  $^{28}\text{SiCl}_4$  with enrichment at 99.99% and the content of impurities of common chemical elements (sodium, aluminum, calcium, iron) at  $n \cdot 10^{-5}$  wt. %.

High-purity silicon-28 tetrachloride has been used for the manufacture of preforms and fiber light carriers based on isotopically enriched quartz glass by the MCVD method [64]. Deposition of isotopically enriched silicon dioxide was carried out on a support tube with a natural content of isotopes; isotopically enriched  $^{28}\text{SiF}_4$  with a degree of enrichment in silicon-28 of  $99.99782 \pm 0.00012\%$  was used as a substance for doping with fluorine and reducing the refractive index of the light-reflecting shell. This resulted in obtaining a piece with a light-guiding structure based on isotopically enriched quartz glass, from which the light-guide was extracted. The refractive index profile of the obtained piece was measured, as well as the spectral dependence of the level of optical losses of the light guide based on isotopically enriched silicon-28 dioxide in the range of 900–1,750 nm [64]. Figure 2 shows

the distribution profile of silicon isotopes in a preform based on isotopically enriched  $^{28}\text{SiO}_2$  according to secondary ion mass spectrometry.

The content of silicon isotopes  $^{28}\text{Si}$ ,  $^{29}\text{Si}$ , and  $^{30}\text{Si}$  in the central part of the preform was  $99.89 \pm 0.10\%$ ,  $0.087 \pm 0.080\%$ , and  $0.023 \pm 0.020\%$ , respectively. These results indicate a marked decrease in the content of the isotope of silicon-28 in the preform relative to its content in the starting substances ( $^{28}\text{SiCl}_4$  and  $^{28}\text{SiF}_4$ ) to a level of 99.9%. Most likely this was caused by the diffusion of silicon isotopes  $^{29}\text{Si}$ ,  $^{30}\text{Si}$  from a support quartz tube with a natural isotopic composition of silicon at the stage of the porous layer melting.

Further research in the field of obtaining isotopically enriched substances and materials based on them should be focused on increasing the level of isotopic purity and obtaining samples of binary substances enriched in the basic chemical elements in their composition.

#### Contribution of the authors

The authors contributed equally to this article.

#### Conflict of interests

The authors declare that they have no known competing financial interests or personal relationships that could have influenced the work reported in this paper.

#### References

1. Devyatykh G. G., Bulanov A. D., Gusev A. V., Pohl H.-J. *Doklady Chemistry*. 2001;376(4/6), 47–48. <https://doi.org/10.1023/a:1018864208808>

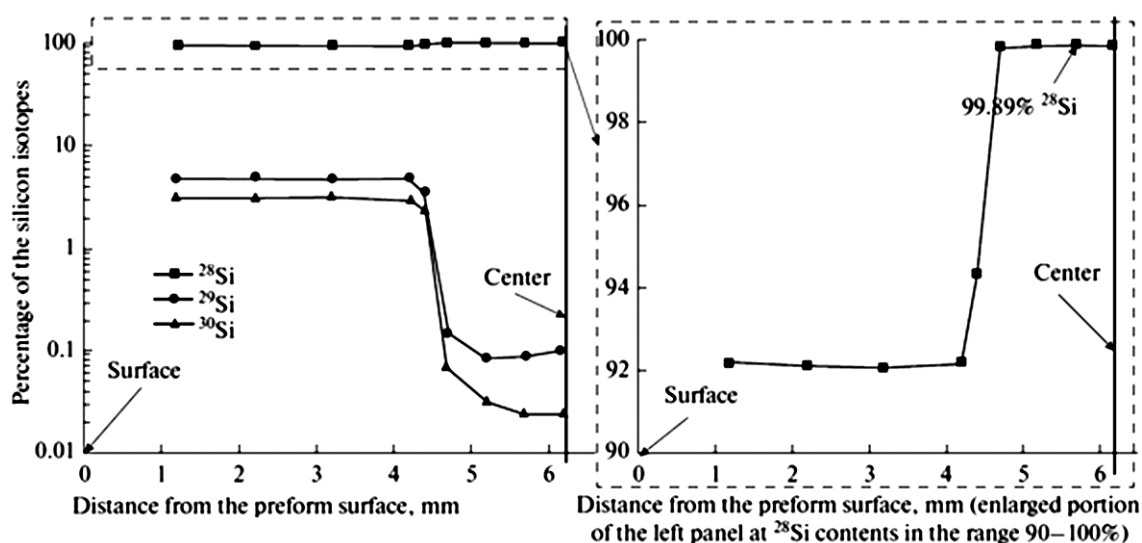


Fig. 2. The distribution profile of silicon isotopes in a preform based on isotopically enriched  $^{28}\text{SiO}_2$  [64]

2. *High-purity substances\**. M. F. Churbanov, Yu. A. Karpov, P. V. Zlomanov, V. A. Fedorov (eds.). Moscow: Nauchnyj Mir Publ., 2018. 996 p. (In Russ.)
3. *Isotopes: properties, production, application\**. In 2 volumes. Vol. 1. V. Yu. Baranov (ed.). Moscow: Fizmatlit Publ., 2005. 600 p. (In Russ.)
4. Plekhanov V. G. Isotope engineering. *Physics-Uspeski*. 2000;170(11): 1245–1252. <https://doi.org/10.1070/pu2000v043n11abeh000264>
5. Itoh K. M., Kato J., Uemura M., ... Rieman H. High purity isotopically enriched  $^{29}\text{Si}$  and  $^{30}\text{Si}$  single crystals: isotope separation, purification, and growth. *Japanese Journal of Applied Physics*. 2003;42: 6248–6251. <https://doi.org/10.1143/JJAP.42.6248>
6. Devyatykh G. G., Bulanov A. D., Gusev A. V., ... Abrosimov N. V. High-purity single-crystal monoisotopic silicon-28 for precise determination of Avogadro's number. *Doklady Chemistry*. 2008(421): 157–160. <https://doi.org/10.1134/S001250080807001X>
7. Abrosimov N. V., Aref'ev D. G., Becker P., ... Zakel S. A new generation of 99.999 % enriched  $^{28}\text{Si}$  single crystals for the determination of Avogadro constant. *Metrologia*. 2017;54: 599–609. <https://doi.org/10.1088/1681-7575/aa7a62>
8. Arefiev D. G., Bulanov A. D., Vasin S. A., ... Churbanov M. F. *Method for separating germanium isotopes\**: RF Patent: No. 2412747. Publ. 02.27.2011, bull. No. 6. (In Russ.)
9. Churbanov M. F., Gavva V. A., Bulanov A. D., ... Gusev A. V. Production of germanium stable isotopes single crystals. *Crystal Research and Technology*. 2017;52(4): 1700026. <https://doi.org/10.1002/crat.201700026>
10. Seyfried P., Spieweck F., Bettin H., ..., Holm C. The silicon-28 path to the Avogadro constant – first experiments and outlook. *Proceedings of Conference on Precision Electromagnetic Measurements Digest*. 1995;44(2): 522–525. <https://doi.org/10.1109/CPEM.1994.333372>
11. Takyu K., Itoh K. M., Oka K., Saito N., Ozhogin V. I. Growth and characterization of the isotopically enriched  $^{28}\text{Si}$  bulk single crystal. *Japanese Journal of Applied Physics*. 1999;38: L1493–L1495. <https://doi.org/10.1143/jjap.38.L1493>
12. Capinski W. S., Maris H. J., Bauser E., Silier ... Gmelin E. Thermal conductivity of isotopically enriched Si. *Applied Physics Letters*. 1997;71(15): 2109–2111. <https://doi.org/10.1063/1.119384>
13. Kremer R. K., Graf K., Cardona M., Gusev A. V., Inyushkin A. V., Taldenkov A. Thermal conductivity of isotopically enriched  $^{28}\text{Si}$ : revisited. *Solid State Communications*. 2004;131: 499–503. <https://doi.org/10.1016/j.ssc.2004.06.022>
14. Gusev A. V., Gavva V. A., Kozyrev E. A., Potapov A. M., Plotnichenko V. G. Preparation of single-crystal  $^{29}\text{Si}$ . *Inorganic Materials*. 2011;47(7): 691–693. <https://doi.org/10.1134/s0020168511070119>
15. Nakabayashi Y., Segawa T., Osman H. I., ... Abe T. Epitaxial growth of pure  $^{30}\text{Si}$  layers on a natural Si(100) substrate using enriched  $^{30}\text{SiH}_4$ . *Japanese Journal of Applied Physics*. 2000;39(11B): L1133–L1134. <https://doi.org/10.1143/JJAP.39.L1133>
16. Inyushkin A. V., Taldenkov A. N., Gusev A. V., Gibin A. M., Gavva V. A., Kozyrev E. A. Thermal conductivity of the single-crystal monoisotopic  $^{29}\text{Si}$  in the temperature range 2.4–410 K. *Physics of the Solid State*; 2013;55(1): 235–239. <https://doi.org/10.1134/s1063783413010150>
17. Becker P., Schiel D., Pohl H.-J., ... Dianov E. M. Large-scale production of highly enriched  $^{28}\text{Si}$  for the precise determination of the Avogadro constant. *Measurement Science and Technology*. 2006;17: 1854–1860. <https://doi.org/10.1088/0957-0233/17/7/025>
18. Andreas B., Azuma Y., Bartl G., ... Zakel S. Counting the atoms in a  $^{28}\text{Si}$  crystal for a new kilogram definition. *Metrologia*. 2011;48: S1–S13. <https://doi.org/10.1088/0026-1394/48/2/S01>
19. Chuprov L. A., Sennikov P. G., Tokhadze K. G., Ignatov S. K., Schrems O. High-resolution Fourier-transform IR spectroscopic determination of impurities in silicon tetrafluoride and silane prepared from it. *Inorganic Materials*. 2006;42(8): 924–931. <https://doi.org/10.1134/s0020168506080231>
20. Krylov V. A., Sorochkina T. G. Gas-chromatographic determination of C1–C4 hydrocarbon trace impurities in silicon tetrafluoride. *Journal of Analytical Chemistry*. 2005;60(12): 1125–1128. <https://doi.org/10.1007/s10809-005-0254-z>
21. Bulanov A. D., Sennikov P. G., Krylov V. A., ... Troshin O. Yu. (2007). Hydrocarbon impurities in  $\text{SiF}_4$  and  $\text{SiH}_4$  prepared from it. *Inorganic Materials*. 2007;43(4): 364–368. <https://doi.org/10.1134/s0020168507040061>
22. Pimenov V. G., Bulanov A. D. Analysis of high-purity silicon tetrafluoride by atomic-emission method with concentration of impurities by matrix sublimation. *Analitika i kontrol'*. 2004; 8(4): 315–321. (In Russ.). Available at: <https://elar.urfu.ru/bitstream/10995/57605/1/aik-2004-04-02.pdf>
23. Bulanov A. D., Pimenov V. G. Determination of impurities in monoisotopic silicon tetrafluoride. *Inorganic Materials*. 2004;40(7): 754–759. <https://doi.org/10.1023/b:inma.0000034777.13686.f8>
24. Kovalev I. D., Potapov A. M., Bulanov A. D. Measurement of the isotopic composition of the isotopic enriched silicon and its volatile compounds by laser ionization mass spectrometry. *Mass-spektrometriya*. 2004; 1(1): 37–44. (In Russ., abstract in Eng.). Available at: <https://elibrary.ru/item.asp?id=9290214>
25. Bulanov A. D., Troshin O. Yu., Balabanov V. V. Synthesis of high-purity calcium hydride. *Russian Journal of Applied Chemistry*. 2004;77(6): 875–877. <https://doi.org/10.1023/b:rjac.0000044107.80122.61>
26. Bulanov A. D., Balabanov V. V., Pryakhin D. A., Troshin O. Yu. Preparation and fine purification of  $\text{SiF}_4$  and  $^{28}\text{SiH}_4$ . *Inorganic Materials*. 2002;38(3): 283–287. <https://doi.org/10.1023/A:1014735203351>
27. Arefiev D. G., Bulanov A. D., Vasin S. A., ... Churbanov M. F. *Method for separating germanium isotopes\**: Patent RF No. 2412747. Publ. 02.27.2011, bull. No. 6.
28. Troshin O. Yu., Bulanov A. D., Mikheev V. S., Lashkov A. Yu. Mechanically activated synthesis of monosilane by the reaction of calcium hydride with silicon tetrafluoride. *Russian Journal of Applied Chemistry*. 2010;83(6): 984–988. <https://doi.org/10.1134/S1070427210060108>
29. Bulanov A. D., Sennikov P. G., Sozin A. Yu., Lashkov A. Yu., Troshin O. Yu. Formation of impurity  $\text{Si}_2\text{OH}_6$  in silane synthesized from silicon tetrafluoride. *Russian Journal*

- of *Inorganic Chemistry*. 2011;56(4): 510–512. <https://doi.org/10.1134/S0036023611040061>
30. Bulanov A. D., Moiseev A. N., Troshin O. Yu., Balabanov V. V., Isaev D. V. Fine purification of monoisotopic silanes  $^{28}\text{SiH}_4$ ,  $^{29}\text{SiH}_4$  and  $^{30}\text{SiH}_4$  via distillation. *Inorganic Materials*. 2004;40(6): 555–557. <https://doi.org/10.1023/b:inma.0000031984.83652.87>
31. Gusev A. V., Bulanov A. D. High-purity silicon isotopes  $^{28}\text{Si}$ ,  $^{29}\text{Si}$  and  $^{30}\text{SiH}_4$ . *Inorganic Materials*. 2008;44(13): 1395–1408. <https://doi.org/10.1134/S0020168508130013>
32. Gusev A. V., Gavva V. A., Kozyrev E. A., Riemann H., Abrosimov N. V. Crucibles for Czochralski growth of isotopically enriched silicon single crystals. *Inorganic Materials*. 2013;49(12): 1167–1169. <https://doi.org/10.1134/s0020168513120078>
33. Andreas B., Azuma Y., Bartl G., ... Waseda A. An accurate determination of the Avogadro constant by counting the atoms in a  $^{28}\text{Si}$  crystal. *Physical Review Letters*. 2011;106(3): 030801(1-4). <https://doi.org/10.1103/PhysRevLett.106.030801>
34. Gibin A. M., Devyatykh G. G., Gusev A. V., Kremer R. K., Cardona M., Pohl H.-J. Heat capacity of isotopically enriched  $^{28}\text{Si}$ ,  $^{29}\text{Si}$  and  $^{30}\text{Si}$  in the temperature range  $4\text{ K} < T < 100\text{ K}$ . *Solid State Communications*. 2005;133(9): 569–572. <https://doi.org/10.1016/j.ssc.2004.12.047>
35. Plotnichenko V. G., Nazaryants V. O., Kryukova E. V., ... Dianov E. M. Refractive index spectral dependence, Raman spectra, and transmission spectra of high-purity  $^{28}\text{Si}$ ,  $^{29}\text{Si}$ ,  $^{30}\text{Si}$ , and Sinat single crystals. *Applied Optics*. 2011;50(23): 4633–4641. <https://doi.org/10.1364/AO.50.004633>
36. Ramdas A. K., Rodriguez S., Tsoi S., Haller E. E. Electronic band gaps of semiconductors as influenced by their isotopic composition. *Solid State Communications*. 2005;133(11): 709–714. <https://doi.org/10.1016/j.ssc.2004.12.038>
37. Sanati M., Estreicher S. K., Cordona M. Isotopic dependence of the heat capacity of c-C, Si, and Ge: An ab-initio calculation. *Solid State Communications*. 2004;131: 229–233. <https://doi.org/10.1016/j.ssc.2004.04.043>
38. Cardona M., Ruf T. Phonon self-energies in semiconductors: Anharmonic and isotopic contributions. *Solid State Communications*. 2001;117: 201–212. [https://doi.org/10.1016/S0038-1098\(00\)00443-9](https://doi.org/10.1016/S0038-1098(00)00443-9)
39. Wille H.-C., Shvyd'ko Yu. V., Gerdau E., ... Zegenhagen J. Anomalous isotopic effect on the lattice parameter of silicon. *Physical Review Letters*. 2002;89: 285901. <https://doi.org/10.1103/PhysRevLett.89.285901>
40. Cardona M., Thewalt M. L. W. Isotope effects on the optical spectra of semiconductors. *Reviews of Modern Physics*. 2005;77: 1173–1223. <https://doi.org/10.1103/RevModPhys.77.1173>
41. Haller E. E. Isotopically controlled semiconductors. *Solid State Communications*. 2005;133(11): 693–707. <https://doi.org/10.1016/j.ssc.2004.12.021>
42. Gavva V. A., Troshin O. Yu., Adamchik S. A., ... Bulanov A. D. Preparation of single-crystal isotopically enriched  $^{70}\text{Ge}$  by a hydride method. *Inorganic Materials*. 2022;58(3): 246–251. <https://doi.org/10.1134/s0020168522030050>
43. Sozin A. Yu., Krylov V. A., Chernova O. Yu., ... Lashkov A. Yu. Study of the impurity composition of isotope enriched german  $^{70}\text{GeH}_4$  by the method of gas chromatography-mass spectrometry. *Perspektivnye Materialy*. 2022;2: 70–82. <https://doi.org/10.30791/1028-978x-2022-2-70-82>
44. Potapov A. M., Kurganova A. E., Bulanov A. D., Troshin O. Yu., Zyryanov S. M. Isotope analysis of  $^{72}\text{GeH}_4$ ,  $^{73}\text{GeH}_4$ ,  $^{74}\text{GeH}_4$ , and  $^{76}\text{GeH}_4$  monogermanes by inductively-coupled plasma high-resolution mass spectrometry (ICP-MS). *Journal of Analytical Chemistry*. 2016;71(7): 667–675. <https://doi.org/10.1134/s1061934816050087>
45. Churbanov M. F., Gavva V. A., Bulanov A. D., ... Abrosimov N. V. Production of germanium stable isotopes single crystals. *Crystal Research and Technology*. 2017;52(4): 1700026. <https://doi.org/10.1002/crat.201700026>
46. Gavva V. A., Bulanov A. D., Kut'in A. M., Plekhovich A. D., Churbanov M. F. Melting point of high-purity germanium stable isotopes. *Physica B: Condensed Matter*. 2018;537: 12–14. <https://doi.org/10.1016/j.physb.2018.01.056>
47. Kut'yin A. M., Plekhovich A. D., Gavva V. A., Bulanov A. D. Development of an applied version of the Kolmogorov–Johnson–Meyl crystallization theory for processing thermal analysis data on the melting temperature and enthalpy of germanium isotopes. *Doklady Rossijskoj Akademii Nauk. Himiya, Nauki o Materialah*. 2024;516(1):30-38. <https://doi.org/10.31857/S2686953524030046>
48. Gibin A. M., Abrosimov N. V., Bulanov A. D., Gavva V. A. Thermal conductivity of single-crystals isotopically enriched  $^{70}\text{Ge}$ ,  $^{72}\text{Ge}$ ,  $^{74}\text{Ge}$  in the temperature range of 80–310 K. *Physics of the Solid State*. 2023;65(8): 1393–1396. <https://doi.org/10.21883/FTT.2023.08.56167.65>
49. Kropotov G. I., Kaplunov I. A., Rogalin V. E., Shakhmin A. A., Bulanov A. D. Particular of radiation transmission of monoisotopic germanium single crystals in the terahertz spectral range. *Applied Physics (Prikladnaya Fizika)*. 2024(1): 80–83. <https://doi.org/10.51368/1996-0948-2024-1-80-84>
50. Lipskiy V. A., Kotereva T. V., Bulanov A. D., Gavva V. A., Churbanov M. F., Nazaryants V. O., Koltashev V. V., Plotnichenko V. G. Refractive index spectral dependence, Raman spectra, and transmission spectra of high-purity  $^{72}\text{Ge}$ ,  $^{73}\text{Ge}$ ,  $^{74}\text{Ge}$ ,  $^{76}\text{Ge}$ , and  $^{nat}\text{Ge}$  single crystals. *Applied Optics*. 2019;58(27): C. 7489–7496. <https://doi.org/10.1364/AO.58.007489>
51. Kropotov G. I., Bulanov A. D., Rogalin V. E., Kaplunov I. A., Shakhmin A. A. (2023). Dependence of the position of phonon IR absorption bands of germanium isotopes on their mass number. *Doklady Rossijskoj Akademii Nauk. Fizika, Tekhnicheskie Nauki*. 2023;511(1), 10–15. (In Russ., abstract in Eng.). <https://doi.org/10.31857/s2686740023040077>
52. Kaplunov I. A., Rogalin V. E., Filin S. A., Kropotov G. I., Shakhmin A. A., Bulanov A. D. *Method of express analysis of objective identification of isotopically pure germanium single crystal*. Patent RF: No. 2813061. Publ. 06.02.2024. (In Russ.)
53. Velmuzhova I. A., Koshelev M. A., Velmuzhov A. P., Ulenikov O. N., Gromova O. V. Thermodynamic functions of germane isotopologues  $^A\text{GeH}_4$  ( $A = 70, 72, 73, 74, 76$ ) calculated from high-resolution IR spectra. *Journal of Molecular Spectroscopy*. 2024;402: 111914. <https://doi.org/10.1016/j.jms.2024.111914>
54. Fedorov A. K. Quantum technologies: from scientific discoveries to new applications. *PHOTONICS Russia*.



2019;13(6): 574–583. (In Russ., abstract in Eng.). <https://doi.org/10.22184/1993-7296.FRos.2019.13.6.574.583>

55. Fedorov A. K., Akimov A. V., Biamonte J. D., ... Zheltikov A. M. Quantum technologies in Russia. *Quantum Science and Technology*. 2019;4: 40501. <https://doi.org/10.1088/2058-9565/ab4472>

56. Valiev K. A. Quantum computers and quantum computations. *Uspekhi Fizicheskikh Nauk*. 2005;175(1):, 3. <https://doi.org/10.3367/ufnr.0175.200501a.0003>

57. Vrijen R., Di Vincenzo D. Electron spin resonance transistor for quantum computation in silicon-germanium heterostructure. *Physical Review A*. 2000;62: 012306(1–10). <https://doi.org/10.1103/PhysRevA.62.012306>

58. Troshin O. Yu., Gavva V. A., Lashkov A. Yu., ... Bulanov A. D. Isotopically modified silicon, germanium and their hydrides for the development of quantum computing devices\*. *Neorganicheskie materialy*. 2023;59(11): 1201–1210. <https://doi.org/10.31857/S0002337X23110143>

59. Heitmann W., Klein K. F. *Glass for optical waveguides or the like*. US Patent: No. 6490399. Published 03.12.2002.

60. Kelsey V., Alexander J.E., Burden S.J. *Isotopically engineered optical materials*. US Patent: No. 20030039865. Publ. 27.02.2003.

61. Churbanov M. F., Bulanov A. D., Troshin O. Yu., Grebenkov K. S. *Method for producing isotopically enriched silicon tetrachloride\**. R F Patent: No. 2618265. Publ. 03.05.2017, bull. No. 13.

62. Troshin O. Yu., Bulanov A. D., Kirillov Yu. P., ... Ermakov A. A. Preparation of high-purity silicon-28 tetrachloride from silicon-28 tetrafluoride. *Inorganic*

*Materials*. 2022;58(8): 854–859. <https://doi.org/10.1134/s002016852208012x>

63. Troshin O. Yu., Bulanov A. D., Chernova O. Yu. Liquid–vapor equilibria in the  $\text{SiCl}_{4-n}\text{F}_n$  ( $n = 1–4$ ) impurity) systems. *Inorganic Materials*. 2018;54(8): 840–843. <https://doi.org/10.1134/s0020168518080162>

64. Troshin O. Yu., Bulanov A. D., Salgansky M. Yu., ... Drozdov M. N.  $^{28}\text{SiO}_2$ -based isotopically enriched silica fiber. *Inorganic Materials*. 2023;59(6): 591–596. <https://doi.org/10.1134/s0020168523060158>

\* Translated by author of the article

## Information about the authors

*Andrey D. Bulanov*, Corresponding Member of the Russian Academy of Sciences, Dr. Sci (Chem.), Chief Researcher, Devyatykh Institute of Chemistry of High-Purity Substances, Russian Academy of Sciences (Nizhny Novgorod, Russian Federation).

<https://orcid.org/0000-0001-5717-0527>  
bulanov@ihps-nnov.ru

*Vladimir A. Gavva*, Cand. Sci. (Chem.), Leading Researcher, Devyatykh Institute of Chemistry of High-Purity Substances, Russian Academy of Sciences (Nizhny Novgorod, Russian Federation).

<https://orcid.org/0000-0003-3071-8884>  
gavva@ihps-nnov.ru

*Oleg Yu. Troshin*, Cand. Sci. (Chem.), Senior Researcher, Devyatykh Institute of Chemistry of High-Purity Substances, Russian Academy of Sciences (Nizhny Novgorod, Russian Federation).

<https://orcid.org/0000-0001-6996-1561>  
troshin@ihps-nnov.ru

Received 05.07.2024; approved after reviewing 24.09.2024; accepted for publication 15.10.2024; published online 25.03.2025.

Translated by Irina Charychanskaya